SIMULATION OF FATIGUE CRACK PROPAGATION RATES IN SMOOTH BENDING SPECIMENS, FROM THE ONSET OF LOADING, USING THE TWO-TERM MODEL

H. Saguy[1], M.P. Weiss[2] and D. Rittel[2]

[1] Rafael Inc., P.O.Box 2250, Haifa 31021, Israel
[2] Faculty of Mechanical Engineering, Technion
Haifa 32000, Israel

ABSTRACT

The fatigue growth of cracks emanating from smooth specimens with stress concentration was investigated. A two-term model of fatigue for step-by-step evaluation of crack propagation from very short cracks to fracture was used to predict the crack growth. Base metal of T1 steel (ASTM 514F) was tested. Growth rates were monitored using the Direct Current Potential Drop method. System calibration was made using an accurate model of the specimen and a numerical solution of the Laplace equation for the electric potential. The two-term model is presented and discussed, and life predictions are compared with experimental results.

KEYWORDS

fatigue modeling, short crack propagation, notches, fatigue diagram

INTRODUCTION

The growth of fatigue cracks based on fracture mechanics, primarily relies on laboratory fatigue tests on specimens containing "long" flaws, which are typically tens of millimeters in length. The continuum approaches, which have been adopted for the characterization of small fatigue flaws, show that the growth rates of small flaws can be significantly greater than the corresponding rates of long flaws when characterized in term of the same nominal driving force [1]. Current design methodology based on linear elastic fracture mechanics (LEFM) provides accurate estimates of fatigue life when the initial size of fatigue flaw is long enough (about half of millimeter). When the material contains defects that are smaller, life predictions nominally based on LEFM may give a non-conservative value (even if small-scale yielding condition prevail). The actual growth characteristics, crack path tortuosity or closure processes for small flaws can be different from those of longer flaws. The problem is further exacerbated by the flaw size detection limit of the non-destructive inspection method. Pearson [2] found that short surface flaws, 0.006 to 0.5 mm deep, grew up to 100 times faster than longer flaws, tens of millimeters in size, which were subjected to the same nominal stress intensity factor range (ΔK). Figure 1 shows a schematic behavior of short crack growth. This figure shows a marked reduction in the rate of growth of the micro-structural short
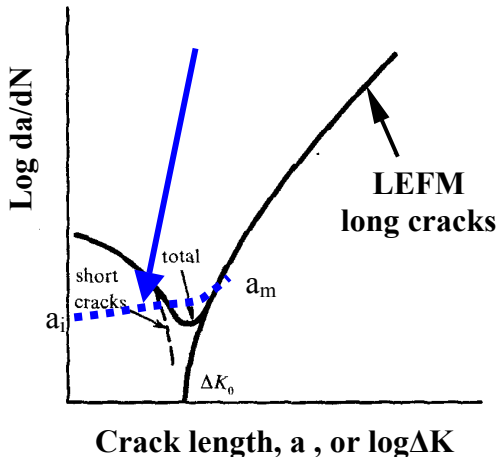
Figure 1: A Schematic of sub-threshold growth of a micro-structurally small fatigue

crack with increasing crack length and when the growth reached the LEFM regime, it starts to increase again as a function of the crack length a.

The growth rate of the retarded short crack subsequently increases with crack length until it merges with the long crack growth data characterized by LEFM. A two-term fatigue life prediction model, from the onset of loading in a smooth specimen until separation by fracture or by gross yielding, has been introduced by one of the authors [3]. The model, based on two terms for crack propagation calculation, has been shown to yield very close fatigue life predictions, compared to experimental results, for AISI 4340 low alloy steel specimens with zero mean stress (i.e. with R=-1) and for block loading with Low-High, and High-Low sequences [4]. In the model a fictitious "equivalent crack" was defined [5] so that the initial micro-crack size - a_i, the intermediate crack size - a_m, and the number of propagating cycles between the two are the same as for the real crack. The fictitious crack rate is monotonic rising. Due to the fact that the size of the intermediate crack a_m, just at the start of the LEFM long crack size is only a few tenths of a mm, one can use the "equivalent crack" for all engineering purposes, and its propagation can be easily simulated with the two term model. Test results from various sources were successfully simulated. The model is based on the assumption that various fatigue mechanisms that have often been observed in fractured fatigue specimens, have been caused by different fatigue regimes. In certain cases, the different regimes exist concurrently in the same fatigue zone and each one causes the crack to propagate independently. In the current study, life predictions are compared with experimental results.

EXPERIMENTAL PROCEDURE

The material used for this study was T1 steel (ASTM 514F) in the form of rolled sheets. T1 steel composition and mechanical properties are presented in tables 1,2. The specimens were machined so as to be parallel to the rolling. The specimens were not machined on the outer surface.

TABLE 1
BASE METAL CHEMICAL COMPOSITION

C	Si	Mn	P	S	Cr	Ni	Mo	V	Ti
0.17	0.22	1.39	0.009	0.001	0.24	0.07	0.48	0.019	0.005

TABLE 2
THE MECHANICAL PROPERTIES OF T1 STEEL

S_y (MPa)	S_{UTS}	Elongation (%)	VHN
780	850	22.4	270

A Keyhole specimen was chosen due to the large amount of experimental data available. This specimen permits studies of both crack initiation and propagation. The crack growth of the specimens was monitored using the Direct Current Potential Drop (DCPD) method. Determination the crack size relies on the principle

that the electrical field in a cracked specimen with a current flowing through it, as a function of the specimen geometry and the crack size. For a constant current flow, the voltage drop across the crack will increase with increasing crack size due to the modification of the electric field. The change in the voltage was translated to crack size using a numeric model and experimental calibration relationship. The numeric model was written using the PDE (Partial Differential Equation) toolbox from Matlab. After drawing the specimen geometry, and defining the boundary condition, the model calculates the Laplace equation. A schematic of the direct current electrical potential crack monitoring system is presented in figure 2.
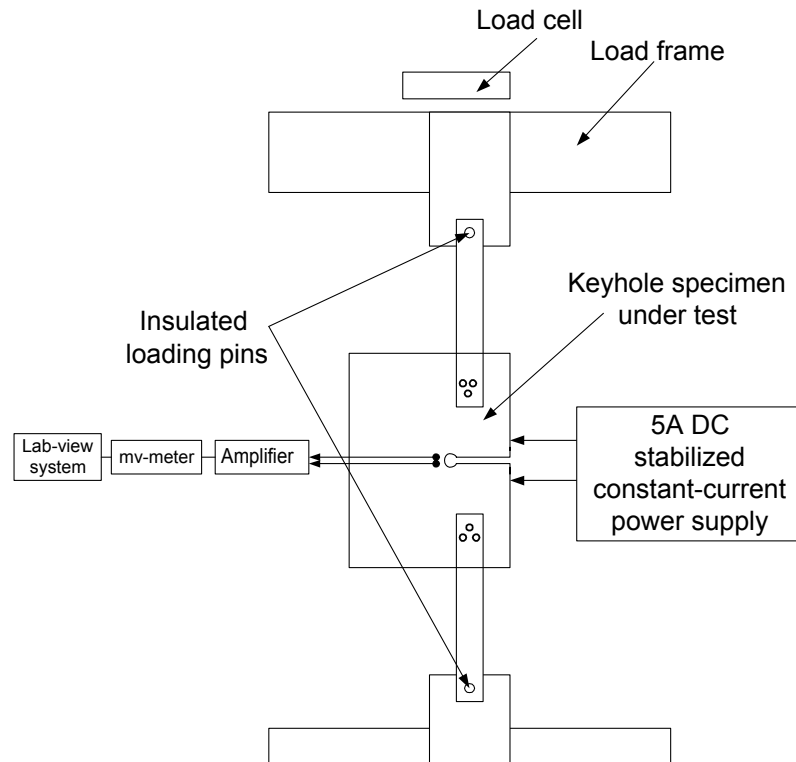

Figure 2: Schematic of the direct current electrical potential crack monitoring system

The specimens were tested under constant amplitude sinusoidal loading at a frequency of 10 Hz. The minimum-maximum load ratio was fixed at R=0.1. The stress intensity factor was calculated separately for short and long cracks and the results were compared with finite element analysis for different crack length.

THE FATIGUE DIAGRAM

The fatigue diagram introduced by Weiss [3,4,] is depicted in Fig 3 and a short description of the zones and regimes follows. The diagram is shown for particular specimen geometry and loading function. For other cases, a different but conceptually similar diagram can be constructed. The diagram covers the whole fatigue domain, starting with the smallest practical micro-cracks (1 micrometers or even less) until the largest and from zero stress amplitude until the ultimate tensile strength. The whole fatigue and fracture domain has been classified, and divided into discrete zones and fatigue regimes, on one comprehensive diagram. Fatigue damage from the onset of loading, is expressed in terms of accumulated crack length, in the whole range of very short, short and long crack ranges. The fatigue domain is divided into six zones by three constant stress amplitudes lines: the endurance limit S_e, the yield strength line S_y, and the ultimate tensile strength S_u, and by two constant stress intensity factor (SIF) lines: the plane strain fracture toughness K_{1c} and the effective threshold SIF range ΔK_{theff}. The use of the diagram helps to explain different fatigue behavior in the same specimen, under different loading regimes, results that in the past were often explained as fatigue scatter. The model that was built based on the diagram, enables to predict the crack propagation quantitatively, cycle by cycle, from the onset of loading, till final fracture. In the very short cracks regime the "equivalent crack" is used instead of the real crack, but for all engineering purposes it is fully adequate.
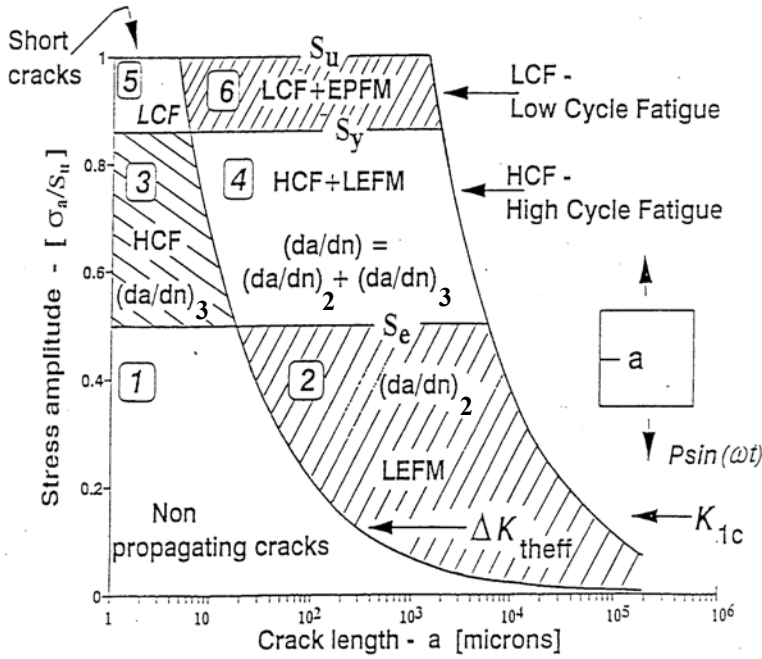
Figure 3: The fatigue domain divided into fatigue and fracture regimes and six zones

The zones differ by the fatigue regimes, as follows:

1. The safe zone. It may contain non-propagating cracks. It lies below both the endurance limit and the effective threshold stress intensity range (below the Kitagawa line).
2. Linear Elastic Fracture (LEFM) regime. Here mostly striation law is a good predictor of experimental results.
3. High cycle fatigue (HCF) regime with very short and short propagating cracks. The classical smooth specimens fatigue tests start here. This is the formerly called crack initiation zone.
4. Both HCF and LEFM regimes are active here concurrently. Crack propagation is formed by a combination of mechanisms and predicted by the superposition, of separately calculated propagation values, for each regime. In this regime most of the industrial failures take place. Here the stress amplitude is higher than the endurance limit and the Stress Intensity Factor range is above the threshold.
5. Low Cycle Fatigue (LCF) regime, very short and short propagating cracks. Parallel to zone 3, but in the plastic range. Industrial structures are not designed here, but pressure vessels are.
6. Both LCF and Elasto Plastic Fracture Mechanics (EPFM) regimes are active here. Crack propagation is formed and can be predicted by a combination of mechanisms. Fatigue understanding in this (and the previous) zones need additional research.

The fatigue diagram makes it possible to designate any cycle of a fatigue test or result, to a certain zone on the diagram, and therefore helps to classify the fatigue experimental domains and compare only test results, when they come from the same zone only. In the past, fatigue results from different zones were used for model evaluation without distinction, and erroneously referred to as fatigue scatter. Real fatigue scatter will thus become much smaller than before, if in the future, valid results will be compared for the same fatigue zone.

SIMULATION

The simulation program calculates the crack increment Δa in each loading cycle. The momentary crack length is calculated as the integration of the crack propagation rate- da/dN, according to the regime on the fatigue diagram where the test takes place. For each stress amplitude and crack length, the program resolves the zone in which crack propagation takes place for that specific loading cycle, and calculates the crack extension for that cycle. The extension is added to the previous depth and so the new crack length is created. The crack growth rate is composed of two separate terms, which depicts the crack growth rate of large cracks above the threshold stress intensity range and cracks at a nominal stress, that are above the endurance limit. A microcrack of 5 μm is assumed to exist. The form of the first crack propagation rate, in the LEFM zone 2, is calculated by the following relation:

$$\left(\frac{da}{dN}\right)_2 = C_1 \cdot \Delta K_{eff}^m \cdot \left(\frac{1-(\Delta K_{th}/\Delta K)^p}{1-(\Delta K/K_{1c})^q}\right) \tag{1}$$

This relation is valid for zone 2 -the LEFM regime only.

The material parameters are C_1 and m (as in the Paris' law). The other term deals with crack propagation due to stress amplitude above the endurance limit. The term $(da/dN)_3$ is defined as:

$$\left(\frac{da}{dN}\right)_3 = C_2 \cdot a^\alpha \cdot \left(\frac{\sigma_a - S_e}{S_u}\right)^n \cdot \left(\frac{1}{1 - (\sigma_a / S_u)^q}\right) \qquad (2)$$

Where C_2, α and q are materials parameters. The parameter N_i has been eliminated and the stress amplitude σ_a introduced. The form of the equation already includes the entire above mentioned boundary effects. The crack rate reaches zero for $\sigma_a = S_e$, and reaches infinity for $\sigma_a = S_u$

The combined relation for crack propagation in specimen or part, under loading conditions for all four zones below the yield strength, is the superposition of eq. (1) and (2), as follows:

$$\left(\frac{da}{dN}\right) = C_1 \cdot \Delta K_{eff}^m \cdot \left(\frac{1 - (\Delta K_{th}/\Delta K)^p}{1 - (\Delta K/K_{1c})^q}\right) + C_2 \cdot a^\alpha \cdot \left(\frac{\sigma_a - S_e}{S_u}\right)^n \cdot \left(\frac{1}{1 - (\sigma_a/S_u)^q}\right) \qquad (3)$$

RESULTS AND DISCUSSION

Experimental fatigue crack growth curve was compared with the simulation prediction. The fatigue crack growh is shown in figure 4.
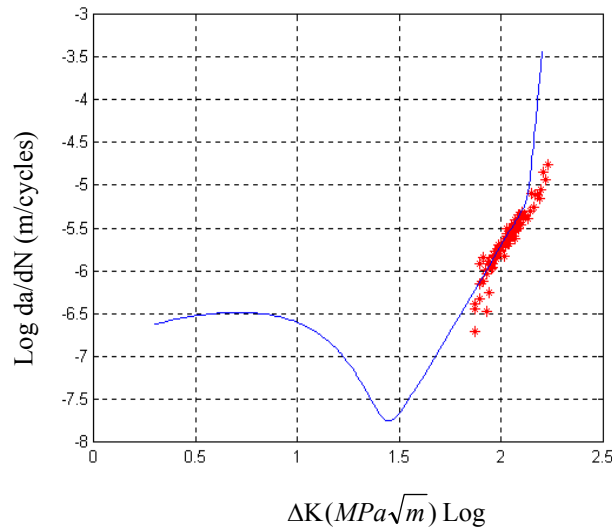

Figure 4: Experimental (stars) and simulated crack (line) propagation rates in a keyhole steel specimen.

The experimental data coincides with the simulation output results at the higher crack sizes. It was not possible to detect cracks below 0.8 mm in the method used. The total fatigue crack growth rate is a sum of the two-fatigue crack growth rates, which suit different zones in the fatigue diagram. The high cycle fatigue crack growth rate $(da/dN)_3$ exhibits crack growth rate beneath the conventional threshold stress intensity range ΔK_{th} and merges with the LEFM crack growth rate $(da/dN)_2$ at the threshold stress intensity range. The experimental results depicted on the fatigue diagram are presented in figure 5. The crack propagates out from the stress concentration, and therefore the line drops down from zone 3 to 4 and then to zone 2. Only after exiting the stress concentration totally, the crack climbs again up to zone 2 and zone 6, where it breaks
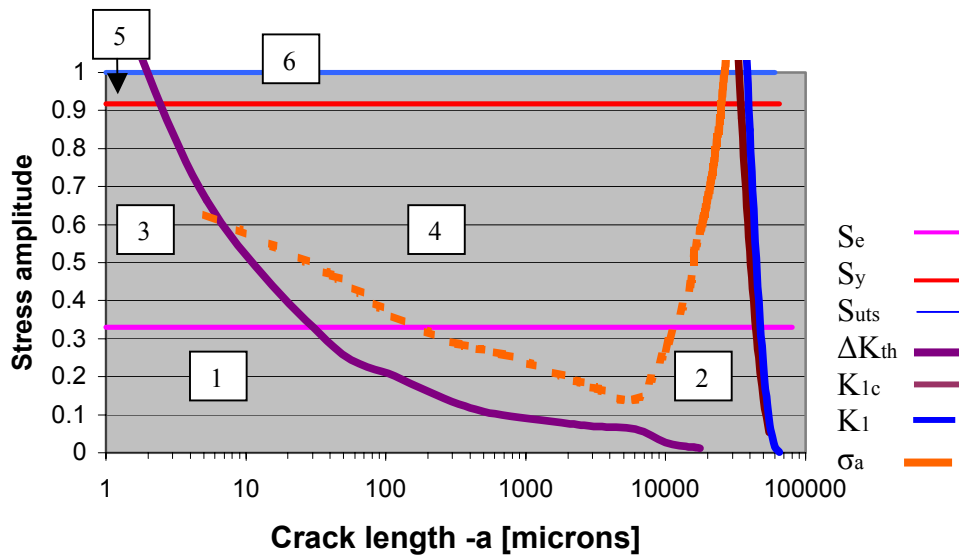
Figure 5 : The Fatigue diagram with the experimental crack propagation line depicted on it

by gross yielding, when reaching the ultimate tensile strength. The line here is unique, because of the large bending stresses in the keyhole type specimen, and it being in plane stress regime

As to the crack propagation rate: as the crack length increased the growth rate decelerated to below the long crack value. After passing through a minimum, the growth rates increased and tended towards the experimental long crack scatter band. As the notch crack extended, the effect of the notch stress field diminished, and led to a reduction on the stress level. On the other hand, as the crack grows the stressed area decreases, and contributes to stress increase. The finite elements analysis for different cracks length also showed a reduction of stress until the crack length reaches 6 mm and then the stress increases. This phenomenon very similar to fatigue cracks behavior, presented in figure 1.

CONCLUSIONS

This study is an additional step in demonstrating the general validity of the fatigue diagram and model, as a practical tool to indicate in which fatigue zone a certain loading cycle takes place and which fatigue regime prevails. It has been shown that a two-term crack propagation equation is a good predictor of fatigue crack propagation.

In our study, the initial detected crack length was of 0.8mm. Measurement of short cracks in the future by visual means is needed in order to compare the results predicted by the model with experimental data.

REFERENCES

1. Suresh S. (1998) : Fatigue of Materials, pp 541-564, Cambridge
2. Pearson, S (1975) "Initiation of fatigue cracks in commercial aluminum alloys and the subsequent propagation of very short cracks". Eng. Fracture Mechanics 7, pp 235-247.
3. Weiss, M.P. (1992) "Estimating fatigue cracks, from the onset of loading, in smooth AISI 4340 specimens, under cyclic stresses", Int J Fatigue **2**, pp 91-96.
4. Weiss M.P. and Hirshberg Z., (1996) "Crack extension under variable loading, in the short and the long crack regime, using a general fatigue diagram", Fatigue Fract. Engng. Mater. Struct. Vol. 19. No 2/3 pp. 241-249. (1996).
5. Weiss M.P. & Peles S.: "Extension of the fatigue two-term model for mean stresses and the crack closure effect", submitted to Engineering Fracture Mechanics.